

Chapter 2

Wireless Power Transfer Based on Metamaterials

Bingnan Wang, William Yerazunis and Koon Hoo Teo

Abstract Near-field-based wireless power transfer (WPT) technology is promising for many applications from consumer electronics to industrial automation. By utilizing resonant coupling, the power transfer can be made more flexible than conventional inductive WPT. However, the range is still limited. In this chapter, we report research work on near-field wireless power transfer (WPT) based on metamaterials-related ideas, aiming to extend the range and improve the flexibility of a WPT system. In the first part, we show that with a thin slab of metamaterial, the near-field coupling between two resonant coils can be enhanced; the power transfer efficiency between coils can also be greatly improved by the metamaterial. The principle of enhanced coupling with metamaterials will be discussed; the design process of metamaterial slabs for WPT will be introduced; experimental results on WPT efficiency improvement with metamaterials will also be presented. In the second part, inspired by metamaterials theory, we study the mutual coupling of an array of coupled resonators, and their application for WPT. We show that the range of WPT can be greatly extended with an array of coupled resonators. More importantly, the technology enables wireless power delivery to both static and mobile devices. The principle of this technology will be explained; analytical and numerical models will be introduced to estimate the performance of a WPT system based on an array of coupled resonators; methods for WPT optimization will be discussed and experimental results will be presented.

B. Wang (✉) · W. Yerazunis · K.H. Teo
Mitsubishi Electric Research Laboratories, 201 Broadway, Cambridge, MA 02139, USA
e-mail: bwang@merl.com

W. Yerazunis
e-mail: yerazunis@merl.com

K.H. Teo
e-mail: teo@merl.com

2.1 Introduction

Wireless power transfer (WPT) has a long history of over 100 years that dates back at least to Tesla in 1893. In recent years, WPT research and product development is reemerging due to rapidly increasing demands in new applications. For example, WPT technology is being deployed to provide wireless charging solutions for batteries of electronic devices including smart phones and wearable devices, which require frequent recharging, and where a mechanical charging socket may wear out in normal use. WPT is promising in many areas with different power levels, from implantable medical devices (usually on the order of milliwatts) to electric vehicles (a few kilowatts to tens of kilowatts). Although each application has specific requirements such as transfer distance, device size, power, and packaging, most of them rely on one of the following fundamental technologies: microwave power transmission, inductive coupling, and resonant coupling.

Microwave power transmission uses directed microwave beams to send energy from transmitting antenna to a receiving antenna. The technology requires accurate alignment and clear line-of-sight and was primarily developed for solar power satellite applications with very high power level, very long distance, and very large investment [1]. It was not typically considered suitable for low power consumer electronics devices charging until recently [2].

In short distance WPT applications, inductive and resonant coupling are two dominating technologies. Inductive method utilizes the inductive coupling between transmitting and receiving coils to transfer power. The efficiency of such a system depends strongly on the coupling coefficient of transmitting and receiving coils. To achieve efficient power transfer, the two coils need to be positioned such that most of the magnetic flux generated by the transmitting coil goes through the receiving coil. Thus inductive coupling-based WPT has a limited power transfer range of a few centimeters and requires precise alignment between transmitting and receiving coils [3–5].

Resonant coupling occurs when the transmitting and receiving coils are tuned to the same resonant frequency. With resonant coupling, the effective transfer distance of a WPT system can be greatly extended [6–12]. Although resonant coupling-based WPT has a long history [6, 7], the application has been very limited. In 2007, Kurs et al. demonstrated that WPT based on resonant coupling can be used to transfer 60 W power over a distance of up to 2 m [8]. This work has since inspired many researchers around the world toward the understanding, analysis, improvement, and application of WPT based on resonant coupling technology (see, for example, Refs. [9–12]).

Using resonance, the system can work efficiently even when the coupling coefficient between transmitting and receiving coils is very small (generally <0.2 , while in the case of inductive coupling, the coupling coefficient is typically >0.9). The efficiency η of a resonant coupling-based WPT system depends on two important factors: the quality factor Q of resonant coils, and the coupling coefficient k between transmitting and receiving coils. Higher Q , which means smaller loss rate in the energy exchange, and higher k , which means higher coupling rate, can both lead to

higher efficiency η [8]. Since the coupling coefficient is directly related to the distance and alignment between transmitting and receiving coils, being able to operate at lower k essentially enables the system to operate at larger distance and in the case of coil misalignment. WPT to a single [8] or multiple [13] receiving devices have been demonstrated at “mid-range” distance, which is several times the characteristic size of the transmitting coil. However, the efficiency still drops rapidly as distance is increasing. It is also desirable to achieve the highest possible efficiency at a given distance for WPT technologies to compete with wired solutions. Since the power receiving devices need to be close to the transmitting device, the mobility is very limited.

In this chapter, we report research on metamaterials for wireless power applications, and show the potential of metamaterials to improve the range and flexibility of WPT systems. In particular, power transfer efficiency improvement using metamaterials, and WPT to mobile devices using array of resonators will be introduced. With a metamaterial slab, the coupling between transmitting and receiving coils can be enhanced, and the efficiency can be subsequently improved [14–19]. In the next section, we will give a brief introduction to metamaterials, their applications to WPT, and a review of recent theoretical and experimental work in this area. With an array of resonators, the range of power transfer can be greatly extended, and dynamic power transfer to mobile devices can be achieved [20–22]. In Sect. 2.3, we will give an introduction to this technology and report experimental development on WPT with arrays of coupled resonators.

2.2 Metamaterials for WPT

Metamaterials are a class of artificially engineered materials which can achieve unique properties that cannot be obtained with natural materials. Metamaterials are typically made from periodic arrangement of structures with unit cell size much smaller than the wavelength at the operating frequency. The properties in response to electromagnetic waves are derived from those engineered structures, instead of the base materials used to build the structures. In the last decade, unique wave phenomena such as negative refractive index and evanescent wave enhancement have been predicted and realized in metamaterials [27–29]. Since the first experimental demonstration of negative index of refraction [28], metamaterials have been shown to be powerful and flexible in achieving desirable electromagnetic properties from radio frequencies to optical frequencies. Numerous applications based on metamaterials have been developed, such as superlens imaging devices [30], invisible cloaking devices [31], and novel antennas [32].

2.2.1 *Metamaterials and Superlens*

The building blocks of metamaterials are engineered structures, typically much smaller in size than the working wavelength, so that metamaterials can be treated as effective media. The electromagnetic properties of a metamaterial are obtained from these building blocks, rather than the composition materials. Macroscopic parameters, such as relative permittivity ϵ , relative permeability μ , and chirality κ can be used to describe the electromagnetic properties of metamaterials. More importantly, we can design for a special set of effective parameters by playing with the shape, geometry, and size of the artificial structures, as these bulk material electromagnetic parameters are determined by those structures in metamaterials. Extraordinary electromagnetic properties, such as negative index of refraction n , which are not readily available in natural materials, have been discovered in metamaterials. Metamaterials have become a powerful tool leading to numerous new discoveries. In 2000, Pendry studied theoretically the wave propagation properties in a negative-index material, and showed that a negative n can be achieved having both ϵ and μ negative in a metamaterial [27]. Negative refraction occurs at the interface between a regular medium of positive n and a negative n metamaterial.

Moreover, while evanescent components decrease exponentially in air or other dielectric media, they can propagate and even be enhanced in a $n < 0$ material. Pendry showed that with a flat slab of metamaterial having the property of relative permittivity and permeability parameters $\epsilon = -1$ and $\mu = -1$, both the far-field propagating waves and the near-field evanescent waves of an object can be restored. This is how the so-called “super lens” is constructed with theoretically unlimited resolution [27]. Although in reality the ideal condition of $\epsilon = -1$ and $\mu = -1$ does not exist, metamaterials designed with physical parameters and low material losses can still achieve imaging resolutions beyond the diffraction limit.

The applications of the unique properties of metamaterials, especially evanescent wave amplification, are not limited to imaging devices. For resonant coupling-based WPT, the power is exchanged between resonators via coupling of near-field evanescent waves [8]. At resonance, electromagnetic fields are confined mostly inside the resonators, and the electric and magnetic fields exchange energy periodically. Outside the resonators, the electromagnetic fields decay evanescently and do not carry away energy, unless coupled to the tail of the evanescent wave of a second resonator. It is thus interesting to see if metamaterials can be applied to WPT systems to improve the coupling, and eventually the power transfer efficiency.

2.2.2 *Metamaterials and WPT*

The adoption of a “super-lens” for near-field WPT was proposed in Ref. [14]. A metamaterial slab of $\epsilon = -1$ and $\mu = -1$ was placed between transmitting and receiving coils in order to study the effect to the near-field coupling. It was shown

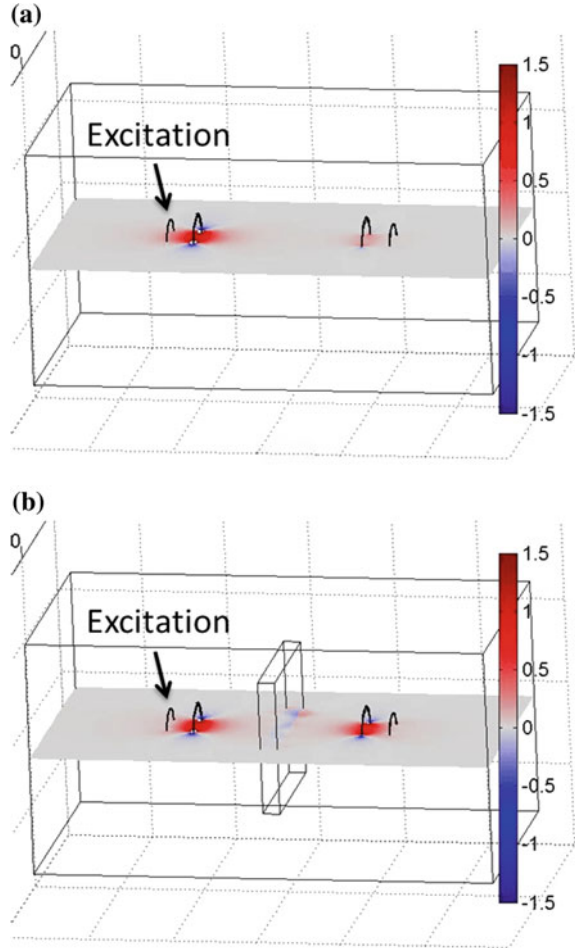
that the metamaterial slab can couple to the near-field evanescent waves, so the effective distance between resonators was reduced, and the coupling coefficient was enhanced. With numerical simulations of a WPT system, it was shown that the power transfer efficiency of the system could also be improved significantly if such a metamaterial slab is used. In Ref. [19], numerical simulations confirmed that the inductive coupling between coils can be enhanced by a metamaterial slab acting as a “super-lens.”

In order to build a “super-lens” metamaterial with negative index for a desired frequency, it is required that both $\varepsilon < 0$ and $\mu < 0$. Two sets of artificial structures are typically needed for the metamaterial to achieve such properties, which is relatively complicated in both design and fabrication. Fortunately, the requirements can be simplified for WPT systems, where the wavelength at the operating frequency is on the order of meters and is much larger than the coil size. Indeed, when we are in the deep subwavelength limit, electric and magnetic field decouple, and only one parameter of ε and μ needs to be negative to make a “super lens” [27]. Depending on if the near-field is dominated by electric field or magnetic field, only $\varepsilon < 0$ or $\mu < 0$ is required. In a WPT system, power is transferred via the coupling of near-field magnetic field, thus a $\mu < 0$ metamaterial is sufficient to achieve the same effect of efficiency improvement [16].

To demonstrate the idea, a four-coil WPT system [8] was modeled and simulated, as shown in Fig. 2.1. Power is injected through the nonresonant loop antenna on the far left side, which is coupled to a nearby resonant coil. The resonant coil is coupled to the receiving side with another coil of the same resonant frequency, which is then inductively coupled to a nonresonant loop antenna at the far right, which is connected to a resistive load. Figure 2.1a shows the simulated magnetic field distribution of the system. The field intensity is strongest at the resonant coil on the left side, due to the excitation of resonant mode. The magnetic field is coupled to the second resonant coil on the right side, but with weaker intensity, due to the large distance in between. In Fig. 2.1b, a metamaterial slab with $\mu = -1 + 0.05i$ and $\varepsilon = 1$ is placed in between the two resonant coils, and the field distribution is shown at the same scale as Fig. 2.1a. While the field intensity at the transmitting coil is the same, the field is seen to be enhanced at the metamaterial slab, and the field intensity at the right receiving resonant coil is increased. It indicates that the metamaterial slab can couple to the near-field evanescent waves, such that the effective distance between resonators is reduced, and the coupling is enhanced.

In Ref. [15], theoretical studies were performed based on an analytical model of the coupling between two coils and a homogeneous metamaterial slab. The coils were simplified as point magnetic dipoles, and the metamaterial slab was assumed to be infinitely large. The coupling between two coils was represented by the mutual inductance L_{21} , and the power transfer was characterized by a simplified circuit model. It was found that the power transfer efficiency from one dipole to the other is proportional to $|L_{21}|^2$. The mutual inductance was calculated taking the ratio of the magnetic flux through the second coil generated by the first current carrying coil and the current magnitude of the first coil. That magnetic flux was calculated by solving the field in the system generated by the first coil. A large slab of metamaterial

Fig. 2.1 Simulated magnetic field distribution of coupled resonators **a** without and **b** with a metamaterial slab. The metamaterial slab has a relative permittivity of -1 and a relative permeability of -1 . The system is excited by a port on the *left side*, and power is transferred to a resistive load connected to the loop antenna on the *right side*



was embedded in the space between the two magnetic dipoles, with the effective ϵ and μ assumed to be homogeneous and uniaxial. The presence of the metamaterial modified the field in the system, thus changed the mutual inductance between coils, as well as the self inductance of the coils. With a metamaterial slab acting as a “super lens,” the mutual inductance can be increased significantly depending on the effective parameters of the metamaterial. Consequently the power transfer efficiency can be improved by the metamaterial. It was shown that, with a realistic magnetic loss tangent 0.1 of the metamaterial slab, the power transfer efficiency with the slab can be an order of magnitude greater than efficiency without the slab.

2.2.3 Experimental Realization

Previous numerical and analytical studies showed that power transfer efficiency can be improved with metamaterials, through mutual coupling enhancement between coils. However, approximations were used in these studies. In the analytical calculation [15], the coils were assumed to be ideal magnetic dipoles, and the metamaterial slab was considered to be infinitely large and homogeneous. In real systems, the inductance and capacitance of coils are distributed and cannot be treated as magnetic dipoles due to the physical size of coils; the size of metamaterial is finite and the homogeneous parameters are not precise. In the numerical simulation [14], although real coils and finite-sized metamaterial slab were used, the metamaterial parameters were still approximated. It is therefore important to verify the findings with experimental measurements.

In Refs. [16] and [17], experiments on WPT with metamaterial have been done. The metamaterial slab is the essential component for the system. As stated previously, power is transferred via the coupling of near-field magnetic field. Thus a “single-negative” metamaterial with $\mu < 0$ and $\varepsilon > 0$, or a magnetic metamaterial was designed.

Magnetic response of physically realizable metamaterials, including secondary effects such as heating and harmonic generation, is an important branch of metamaterial research. Previously, magnetic metamaterials have found applications in areas including new antennas [32] and magnetic resonance imaging systems [33]. However, most of applications of metamaterial before WPT are for information processing, where the required power level is very low, typically on the order of milliwatts. In a WPT system, depending on target applications, the required power level can be anywhere from a few watts to a few kilowatts. Power handling is a major challenge to the metamaterial design. While loss in metamaterial is less sensitive in information processing, it is critical in WPT systems, where the efficiency needs to be as high as possible in order to compete with wired power delivery. For a typical metamaterial, the ratio of operating wavelength to unit cell size λ/a is 10 or less. However, for WPT, the whole system is usually much smaller than the wavelength, producing a λ/a ratio greater than 100. The required fabrication process needs to be simple and low cost for commercial viability. In summary, the metamaterial for WPT needs to be low loss, low cost, compact, and capable of handling high power.

As shown in the inset of Fig. 2.2a, the building block of the metamaterial are two-sided square spirals. The structure is designed to achieve the compact size and low-loss requirements. The 3-turn spirals are printed on Rogers RO4003C circuit boards, with the two sides connected by vias. With a size 6.5 mm by 6.5 mm, the structure gives strong response to external magnetic field around resonant frequency of 24 MHz. The strong response comes from the resonance of the structure, which can be effectively considered as an LC resonator, where the inductance comes from the multi-turn metal wires, and the capacitance comes mainly from the “plate capacitor” formed by the two sides of metal structure on the printed circuit board. The effective inductance and capacitance are much larger than conventional split-ring resonators of

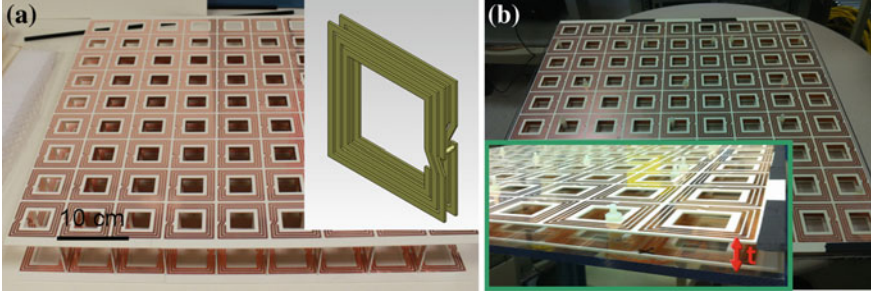


Fig. 2.2 **a** The fabricated 3d metamaterial, with the unit cell structure shown in the inset. **b** A picture of the planar metamaterial, with inset showing the details. t is the spacing between two planes

the same size, so much lower resonant frequency is achieved. In terms of wavelength to unit cell ratio λ/a , the double-sided spiral design is about 170, while conventional split-ring resonator is around 10.

A μ -negative metamaterial can be constructed by assembling these spirals in cubic lattice [16], as shown in Fig. 2.2a. Above the resonant frequency, the effective μ (relative magnetic permeability) of the metamaterial is negative. At our working frequency of 27.12 MHz, this metamaterial has an effective μ very close to -1.0 as well as a relatively simple fabrication, low loss, and compact size.

Metamaterial with a different negative effective μ can also achieve evanescent wave enhancement. However, when the absolute value of negative μ is larger, the frequency gets closer to the resonant frequency of the composing spirals, causing increased Ohmic loss in metallic structures and dielectric loss in the substrate of the metamaterial and less power transfer efficiency improvement.

Other components of a WPT system were also designed and fabricated. This system is intended to work at the ISM band with center frequency of 27.12 MHz. As shown in Fig. 2.3a, two planar coils built with copper wire spirals are used as resonators. Two nonresonant loop antennas are inductively coupled to the resonant coils. RF power is fed to the system by connecting to the loop antenna on the right side. Power is transferred to the left-side resonator and picked up by the second loop antenna, and delivered to a load (an incandescent light bulb).

Experiments were performed to measure the power transfer efficiency of the WPT system at low power [16]. The overall efficiency of the system was measured by an Agilent N5230A vector network analyzer. The two loop antennas were connected to the two ports of the network analyzer, and S-parameters between the two ports were measured. For each measurement, the distances between loop antennas and associated coil resonators were tuned so that the system can be properly matched to the $50\ \Omega$ ports of the network analyzer for optimal power transfer [12, 13]. When a metamaterial slab is added in the system, the optimal condition needs minor adjustment. The distances between loop antennas and associated coil resonators need to be

Fig. 2.3 WPT experiment to a 40 W light bulb of system **a** without metamaterials, **b** with the 3D metamaterial slab, and **c** with the anisotropic metamaterial slab. The separation distance is 50 cm for all cases

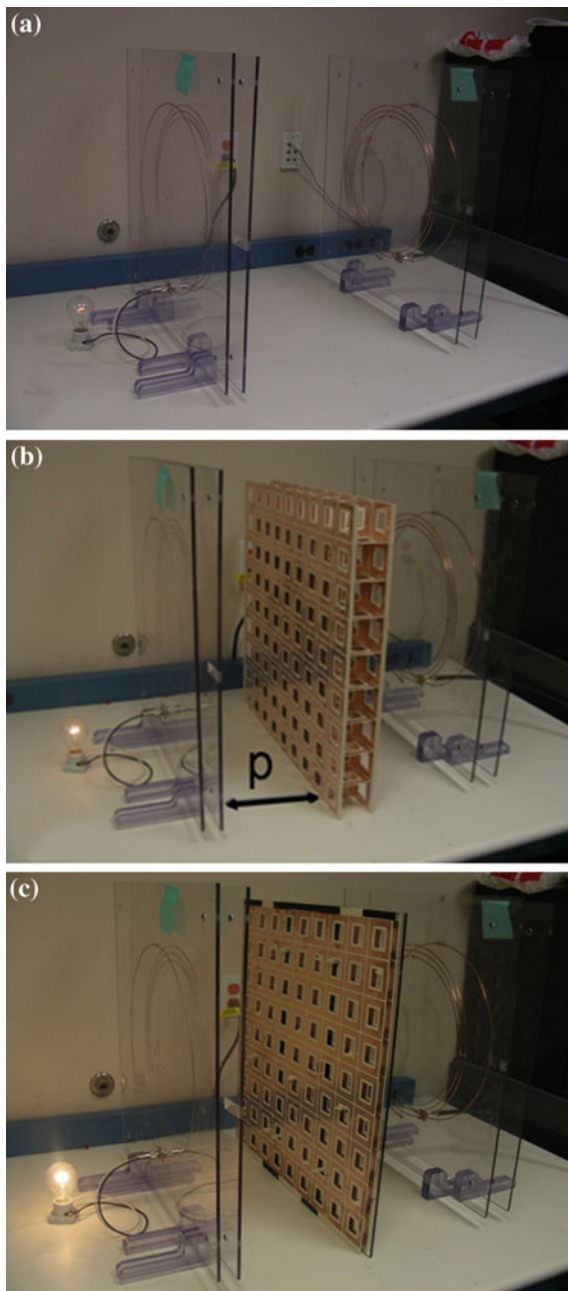
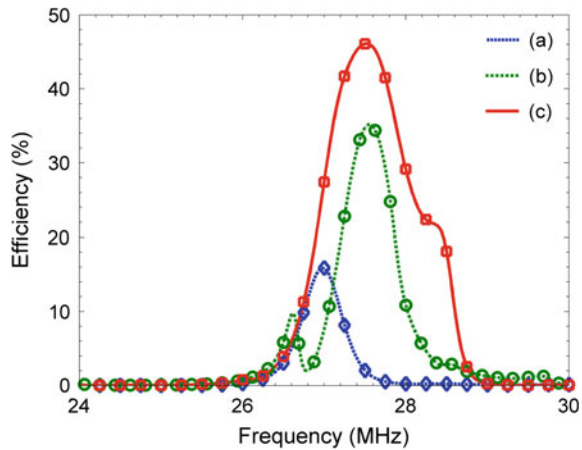


Fig. 2.4 The measured power transfer efficiency of different system configurations: **a** original system without metamaterials, maximum efficiency is 17 %, **b** with a 3D metamaterial slab, maximum efficiency is 35 %, and **c** with an anisotropic metamaterial slab, maximum efficiency is 47 %



readjusted so that the optimal matching for power transfer is achieved. The reflection parameters S_{11} and S_{22} around resonance are both small (around -20 dB), and the change due to the introduction of metamaterial is negligible. Thus the power transfer efficiency of the system can be estimated by $|S_{21}|^2$. At a distance of 50 cm between two resonant coils, the efficiency without a metamaterial is 17 %, and is increased to 35 % with the metamaterial slab in the system [16], as shown in Fig. 2.4.

In Ref. [17], the metamaterial slab for WPT was further simplified. Instead of stacking the two-side square spirals in three dimensions, only two flat panels of spirals were used to construct an anisotropic metamaterial, as shown in Fig. 2.2b. The simplification is made because the magnetic field in the WPT system is mainly in the direction along the axis of the spirals. It is sufficient to use a metamaterial having negative magnetic response in this direction, instead of an isotropic metamaterial. The two surfaces are separated by a distance $t = 2$ cm, optimized to achieve highest power transfer efficiency of the system. With the same method, the efficiency is measured with the anisotropic metamaterial in the WPT system. As shown in Fig. 2.4, the efficiency is increased to 47 % at maximum, comparing to peak efficiency of 17 % without the metamaterial. The achieved efficiency is even higher than the case of isotropic metamaterial, as the loss is lower in the planar metamaterial with unnecessary structures removed. In the anisotropic metamaterial, evanescent wave enhancement is achieved via the excitation of surface waves on the two surfaces. Before WPT, anisotropic metamaterials have been used for near-field imaging [35].

Experiments at higher power level have also been done to the WPT system [16, 17]. Figure 2.3 shows the experimental demonstration of wireless power transfer to a 40 W light bulb. The RF power is provided by a high-frequency transceiver with power amplifier through the input loop antenna. Similar as in the efficiency measurement, the distances between loop antennas and associated resonators are adjusted for optimal matching each time. When a metamaterial slab is inserted in the system, the matching process is repeated to minimize the affect of mismatch. The brightness of

light bulb can thus reflect the amount of power transferred. Figure 2.3a shows the system without metamaterial, where the light bulb barely glows. Figure 2.3b shows the system with the anisotropic metamaterial, and the light bulb is much brighter. This indicates that the efficiency is indeed improved significantly by the metamaterial. The experiment also shows that the metamaterial is capable of handling the high power level.

Later on, the idea on metamaterials for enhanced WPT has been verified by several other studies. In Ref. [23], a “super-lens” metamaterial slab was fabricated for a WPT system, and shown to be capable of increasing the range of power transfer, as well as the power transfer efficiency compared with lensless system. In Ref. [24], improved power transfer efficiency was demonstrated for a short-range telemetry system with a compact metamaterial. The efficiency improvement was achieved with the metamaterial slab placed in close proximity to transmitting or receiving coils. In Ref. [25], the misalignment between transmitting and receiving coils was studied, and it was shown that a metamaterial slab can be applied to mitigate the effect of misalignment and improve the power transfer efficiency. In Ref. [26], a compact metamaterial with adjustable operating frequency between 10 and 30 MHz was designed and fabricated. The metamaterial was applied to a two-coil WPT system and shown to be able to improve the power transfer with less waveform distortion.

2.3 Array of Resonators for Mobile Power Transfer

In a resonant coupling-based WPT system, the basic configuration is to have a pair of resonant coils. Wireless power is transferred between the coil pair through coupling of evanescent waves. The resonant coil can be excited through inductive coupling to (as shown in Fig. 2.5a), or directly collected to an excitation source. Although some flexibility in range can be realized, the region of efficient power transfer is still limited to the physical size of the coils. For devices that travel with distance much larger than the physical size of the transmitting coil, the technology is not sufficient to provide wireless power continuously. Examples include the wireless charging for battery-powered vehicles on the road, wireless power for elevators, or wireless power for industrial robots that can travel a long distance. In this section, we introduce a feasible solution to the problem, and show that by utilizing the coupling of an array of resonators, mobile WPT to multiple mobile devices is achievable [20–22]. With this technology, mobile WPT to electric vehicles on road can be realized. By embedding a power transmitting array of resonators under surface of road or track, power can be picked up wirelessly and continuously by vehicles with pre-installed power receivers traveling on the road.

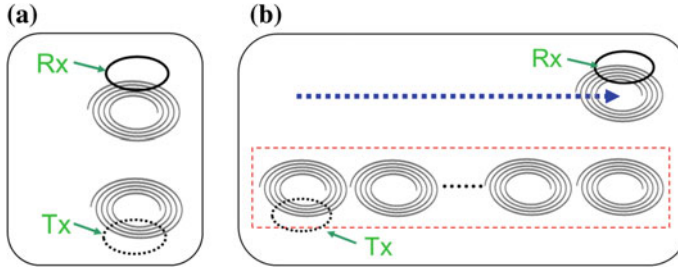


Fig. 2.5 **a** WPT system with one resonant coil as transmitter and one resonant coil as receiver. **b** WPT system with an array of resonant coils as transmitter and one resonant coil as receiver

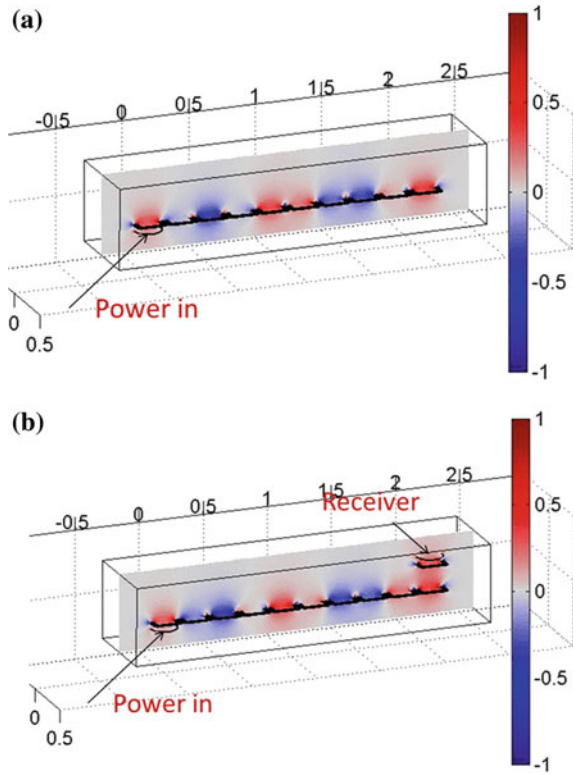
2.3.1 Array of Coupled Resonators

An array of coupled resonators can be formed by multiple resonators with same or similar resonant frequencies when each resonator is resonantly coupled to its neighboring resonators. Figure 2.5b shows a simple example of an array in linear shape, which is composed of multiple coils aligned in a straight line. Of course, the resonator design and the shape of the array can both take different forms [20]. For example, the resonators can be arranged in more complex routes with bends and curves. The key is that, when one resonator in the array is excited by an external source, power can be resonantly coupled to its neighboring resonators, then to the next neighbors, then to all resonators in the array. As shown in Fig. 2.5b, power can be distributed in the array by inductively coupling a loop antenna to the first resonator in the array. When a resonant receiver is close to the array and is coupled to any resonator or resonators in the array, power can be transferred to it. The power is distributed and transferred in the system via resonant coupling, thus no electrical connections between resonators are required. The receiver can also be kept a distance away from the array. Two features of the system can be observed. First, the effective power transfer range is greatly extended, as the receiver can now be anywhere along the array, which can be much larger than the physical size of one resonator. Second, the receiver can be attached to a mobile device and travels along the array freely. It is even possible to allow multiple receivers to be powered by the system at the same time, as long as each receiver is coupled to the array.

2.3.2 Numerical Simulations and Circuit Analysis

A system similar to the one shown in Fig. 2.5b is modeled and simulated in COMSOL. In the model, the resonators are square spirals of width 20 cm, designed to have a resonant frequency around 25 MHz. A linear array is formed by 10 resonators side-by-side. A loop antenna is aligned to the first resonator in the array and inductively

Fig. 2.6 Simulated magnetic field distribution of a WPT system with an array of 10 resonators as transmitter: **a** No receiver, and **b** with receiver



couples the energy to the system. With these settings, the magnetic field distribution of the system is calculated and plotted in Fig. 2.6a. A strong field is excited by the nonresonant loop antenna, and localized around resonators in the array. Now we place another resonant coil and a nonresonant loop antenna as receiver and align them with the 10th resonator of the array. As shown in Fig. 2.6b, even though the receiver is very far from the transmitting antenna, a strong field is still seen at the receiver due to resonant coupling between the resonant receiver and the last resonators in the array. Thus efficient WPT can be achieved over a long distance.

As shown in Fig. 2.6, the field is not uniformly distributed along the array. The coupled mode of the resonator system forms a standing wave on the array, with the phase difference between neighboring resonators depending on the operating frequency. It is therefore important to evaluate the power transfer performance of the system when the receiver is at different positions.

As numerical simulations are time consuming, a transmission line model based on circuit analysis and analytical calculations has been developed to quickly evaluate the performance of the array-based system [21]. In the model, each resonator is treated as a tank circuit; capacitive coupling between resonators is neglected and inductive

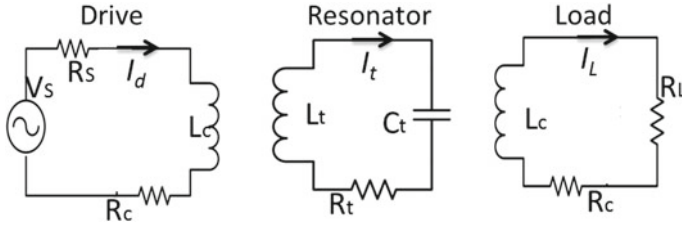


Fig. 2.7 Circuit model for the nonresonant drive coil, resonant coil in the array and receiver, and nonresonant load coil

coupling is quantified by mutual inductances; nonresonant coils, including the drive and load coil, are also modeled as simple RL circuits, as shown in Fig. 2.7.

The inductance, capacitance, resistance and resonant frequency for resonant coils, the inductance and resistance for nonresonant coils, as well as the mutual inductance between coils are calculated analytically based on the geometry and relative positions of coils. For simplicity, we consider all resonant coils in the array and the resonant receiving coil as identical, thus having the same inductance, capacitance, and resistance values. Similarly, the two nonresonant coils for transmitter and receiver are also identical. Also, we assume the mutual inductance between coils depends only on their separation distance, not on their position in the array system. Thus all nearest neighboring couplings in the array is the same. Finally, we assume that the mutual coupling is reciprocal. With these in mind, we can reduce the circuit elements in the system to those listed in Table 2.1. Referring to Fig. 2.5, the resonant receiving coil and nonresonant load coil moves together linearly along the array of N resonant coils, and the position is marked as x relative to the first coil in the array.

The coupled circuits can be represented by a system of equations derived by Kirchhoff's voltage and current laws. The self-impedances for each resonant coil and nonresonant coil are, respectively

$$Z_t = R_t + j(\omega L_t - \frac{1}{\omega C_t}) \quad (2.1)$$

$$Z_c = R_c + j\omega L_c \quad (2.2)$$

For nonresonant drive coil, we have

$$V_s = I_d(Z_c + R_s) + \sum_{m=1}^N j\omega M_{dt}(m)I_m + j\omega M_{dr}(x)I_r + j\omega M_{dL}(x)I_L \quad (2.3)$$

For each resonator in the array, we have an equation of the following form:

$$0 = I_t Z_t + j\omega M_{dt}(t)I_d + \sum_{m=1, m \neq t}^N j\omega M_{tt}(t, m)I_m + j\omega M_{rt}(t, x)I_r + j\omega M_{Lt}(t, x) \quad (2.4)$$

Table 2.1 Symbols and their meanings in the circuit analysis

Symbol	Meaning
R_t, C_t, L_t	Resistance, capacitance, and inductance of a resonant coil
R_c, L_c	Resistance and inductance of a nonresonant coil
V_S, R_S	Voltage source voltage, and resistance
R_L	Load resistance on the load coil
$M_{tt}(m, n)$	Mutual inductance between coils m and n of the array
$M_{dt}(m)$	Mutual inductance between drive coil and resonant coil m of the array
M_{Lr}	Mutual inductance between the receiver coil and load coil
$M_{rt}(m, x)$	Mutual inductance between the receiver coil and resonant coil m of the array when the receiver is at position x
$M_{Lt}(m, x)$	Mutual inductance between the load coil and coil m of the array when the receiver is at position x
$M_{dr}(x)$	Mutual inductance between the receiver coil and the drive coil when the receiver coil is at position x
$M_{dL}(x)$	Mutual inductance between the load coil and the drive coil when the receiver coil is at position x
$I_{d,m,r,L}$	Current in the drive coil, m -th resonant coil in the array, resonant receiving coil, and the nonresonant load coil

For the resonant receiving coil, we have

$$0 = I_r Z_t + j\omega M_{Lr} I_L + j\omega M_{dr}(x) I_d + \sum_{m=1}^N j\omega M_{rt}(m, x) I_m \quad (2.5)$$

And for the nonresonant load coil, we have

$$0 = I_L (Z_c + R_L) + j\omega M_{dL}(x) I_d + j\omega M_{Lr} I_r + \sum_{m=1}^N j\omega M_{Lt}(m, x) I_m \quad (2.6)$$

By solving the system of equations, the current in each coil, the transmitted power $P_t = \frac{1}{2} \Re(V_S \cdot I_t^*)$, the received power at load $\frac{|I_L|^2}{2R_L}$, as well as the power transfer efficiency $\eta = P_L / P_t$, can all be obtained.

For an array with 10 resonators, the power transfer efficiency is calculated as a function of receiver position as well as excitation frequency, and plotted in Fig. 2.8. For a fixed excitation frequency, as the receiver moves from one end to the other end, there are highs and lows in efficiency, and different pattern is seen at different frequencies. This is due to the nonuniform field pattern of coupled modes in the array, and different coupled modes of the array are excited at different frequencies. On the other hand, at a fixed receiver position, very different efficiencies can be obtained depending on the excitation frequency.

Fig. 2.8 Power transfer efficiency (given by circuit analysis) from a 10-resonator array to a receiver, as function of receiver position in unit of lattice size of the array, and the transmitter frequency

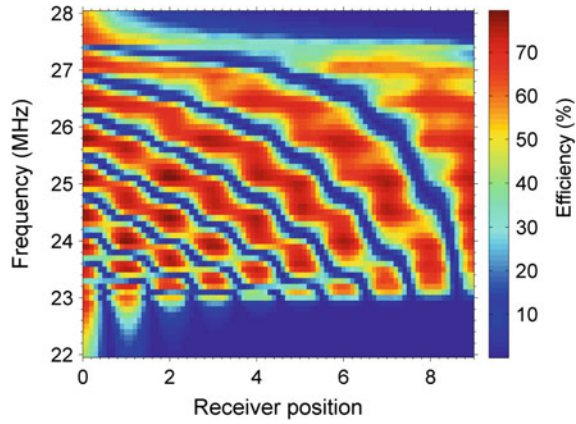
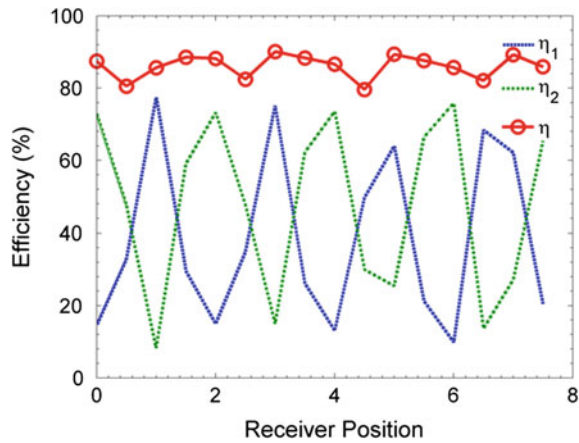


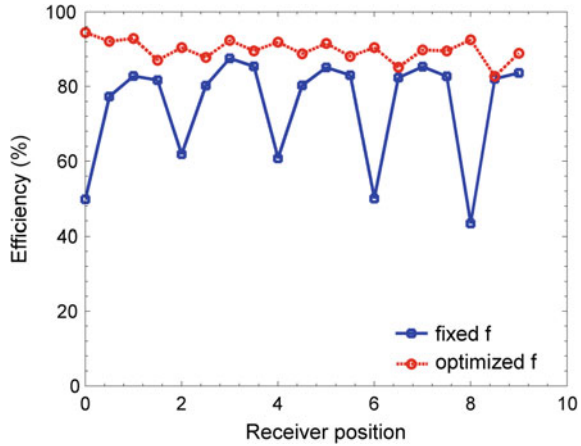
Fig. 2.9 Simulated power transfer efficiency to two individual receivers and the combined efficiency, as functions of receiver position in unit of lattice size of the array. Operating frequency is fixed



In order to improve power transfer performance, the fluctuation in efficiency as a receiver is moving along the array needs to be reduced. In a WPT system with a single resonant transmitter, it has been discovered that the more receivers in the system, the higher the overall efficiency can be achieved [13]. Similarly, the more receivers we have in the array-based system, the higher the efficiency can be obtained. Moreover, the overall efficiency can be more stable compared with a single-receiver case.

Consider the 10-resonator array system in previous simulations, we now use two resonant receivers that are moving simultaneously along the array, with a lateral distance of 10 cm. In this case, the power at each output port is calculated. The ratio of this output power to the input power is taken as the efficiency to each receiver. The overall efficiency is the sum of the two. They are plotted in Fig. 2.9 as functions of lateral position of the first receiver on the array in unit of the lattice size of the array. Although each receiver has significant fluctuation on the efficiency at different positions, the overall efficiency is much more stable.

Fig. 2.10 Simulated power transfer efficiency to one receiver as function of receiver position in unit of lattice size of the array, operating at a fixed frequency (blue) and optimized frequency for each position (red)



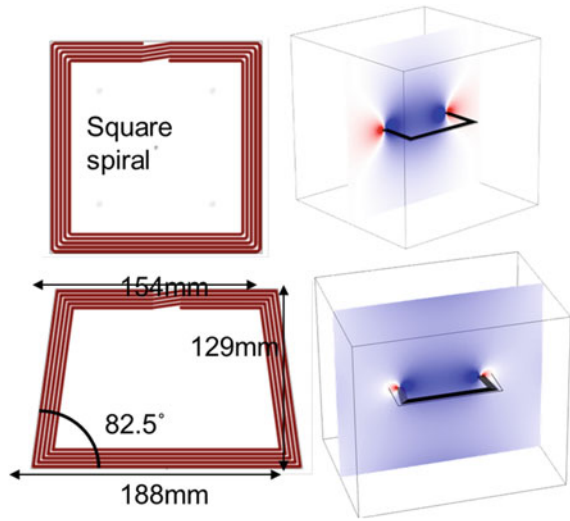
In case of a single receiver, the efficiency fluctuation can be reduced by adjusting the transmitting frequency depending on the position of the receiver. As shown in Fig. 2.8, different efficiencies can be achieved at the same position by changing the frequency. If the frequency is used such that highest efficiency is achieved at each position, the power transfer is optimized for the receiver. Figure 2.10 shows an example of simulated efficiency with a fixed frequency, and optimized frequency for each position, for the same 10-resonator array system used in previous simulations.

To achieve the optimization in real system, a data link can be set up between receiver and transmitter. A monitor can be used on the receiver to detect and send the power transfer status information via the data link back to the transmitter, and the transmitter can then adjust the transmitting frequency depending on the feedback [22].

2.3.3 Experiment Demonstration

To demonstrate the flexibility of the array base WPT, we did an experiment with a toy train set running on an oval-shaped track, and built an array of resonators to follow the track and provide power to the train running above. The oval-shaped track has a dimension of 183 cm by 140 cm, and total length of 5.25 m. Planar spirals on circuit board are used for resonator designs in this study for their simple yet reliable fabrication process. For such planar spiral structures, a semi-analytical model has been developed by Ellstein et al. [36] to quickly obtain their resonant frequencies. Two types of resonators are designed for the straight and curved tracks, respectively. As shown in Fig. 2.11, both types are planar 5-turn spirals printed on 0.5 mm Rogers 4350 circuit board, with copper thickness 35 μm , copper strip width 2 mm, spacing between neighboring copper strips 1 mm. The square-shaped

Fig. 2.11 Design (*left*) and simulated magnetic field distribution at resonance (*right*) of planar resonators for the array experiment



resonator has an outer dimension of 15 cm by 15 cm; the trapezoid-shaped resonator has a height of 12.9 cm and side lengths of 15.4 and 18.8 cm. A total of six square-shaped resonators and 24 trapezoid-shaped resonators are used to fill up the oval-shaped track. Square and trapezoid shapes are used in order to have higher coupling coefficient between neighboring resonators by minimizing the distance between the conductors of adjacent resonators. Low-loss substrate is used to reduce power loss in the system, and the resonators are designed and fabricated with standard printed circuit technology for simple and accurate control of the parameters. Both resonators have self-resonant frequency around 25 MHz. The magnetic field distribution of the resonators is also shown in Fig. 2.11, indicating strong field localization due to the high-Q resonances.

Once the resonators are fabricated, they are placed underneath the oval track, with RF power provided to the array via a square antenna inductively coupled to one of the resonators in the array. To receive power, a resonant coil and a nonresonant loop antenna is placed underneath the coal tender of the train set, about 5 cm above the array. The batteries in the coal tender are removed and replaced by circuits for RF to DC conversion. The converted DC power, typically at a voltage varying between 30 and 170 V, is routed to a 40 W light bulb and to a wide-input switching power supply, which produces +5 V for the locomotive's electric motor. A 2 Farad supercapacitor provides a small amount of load leveling.

Figure 2.12 shows the components of the demonstration system. A Kenwood TS-480 transceiver is modified and used as RF power supply [Fig. 2.12a], which is capable of putting out 200 W power with frequency between 3 and 30 MHz. A nonresonant square loop antenna [Fig. 2.12b] is connected to the RF power supply and provides power to the array system via inductive coupling. An additional test receiver consisting of a square resonant coil, inductively coupled to a loop antenna, which

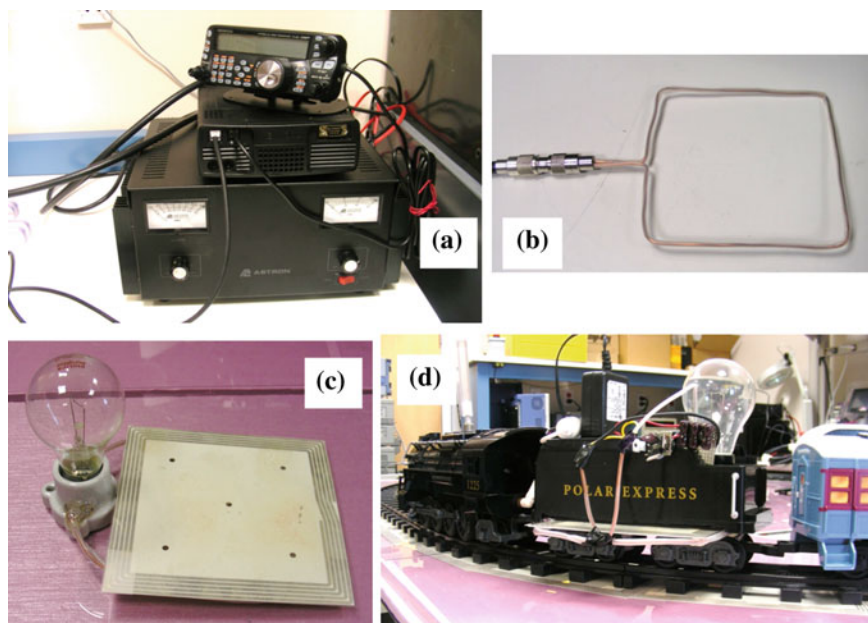


Fig. 2.12 Components of WPT experiment with array of resonators: **a** RF power transmitter; **b** square antenna to inductively couple power from the RF transmitter to the system; **c** a wireless power receiver composed of a resonant coil, a loop antenna and a 40 W light bulb; **d** a wireless power receiver with a resonant coil and a loop antenna to pick up RF power, a rectifier and regulator to convert RF power to DC, and a motor for the toy train set and a 40 W light bulb as load

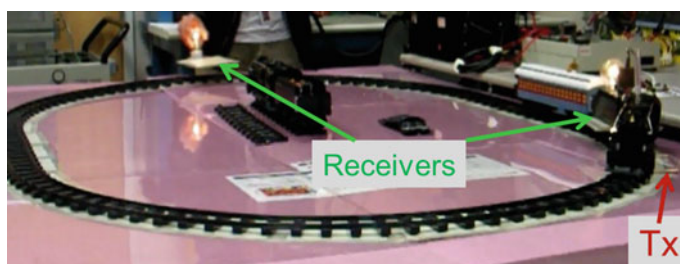


Fig. 2.13 WPT experiment with array of resonators. The system is used to provide power wireless power to two sets of receivers, one of which is the toy train set moving along the track

is then connected to a 40 W light bulb, is used for power receiving experiment and indicating the transferred power level [Fig. 2.12c]. Figure 2.12d shows the modified train set. The array of resonators under the track is visible in the picture.

The above components were assembled and the WPT system was tested. As shown in Fig. 2.13, the square antenna connected to the RF power supply is coupled to one resonator in the array inductively. With an 80 W power output from the RF power supply, the train set is able to run continuously along the oval track with the

wireless power supply. In addition, the light bulb on the train and the one with a separate receiver are both lit up with wireless power. While the train is traveling along the track, the brightness of the light bulb on the train changes, indicating that the power transferred to the receiver varies. As discussed before, this is a result of resonant coupling in the array. A Bird 4410 wattmeter was used to measure the received power. The fluctuation is significant: the efficiency at peak is about 85 % while efficiency at low is about 15 %.

We observed that at many frequencies, the system does not maintain sufficient voltage to operate the locomotive motor at all points in the loop. This is due both to the node and antinode effect as seen in Fig. 2.8, and also because the loop is closed, so energy circulating clockwise and energy circulating counterclockwise interferes both constructively and destructively. Manually changing the frequency shifts the resonant nodes and antinodes and allows adequate power delivery at all points on the loop. Our hypothesis is that this frequency change can be automated, and yield an improved overall energy delivery.

We then implemented a telemetry system on the train that measured the actual voltage on the high-voltage capacitors at approximately 5 Hz and relayed the value in real time to a host Linux laptop via Bluetooth. We then operated the train set at 100 W nominal power from 23 to 25 MHz (the useful resonance band of our test system) and logged the instantaneous power delivered. The experimental protocol was to test several different automatic frequency tuning strategies and compare them versus fixed-frequency systems. Our tuning strategies were allowed freedom within the same 23–25 MHz band as the fixed-frequency standards, and changed frequencies in steps of either 50 or 100 kHz, either automatically or with feedback via the telemetry system.

As a result, every mode of active tuning operated the train on a continuous loop without failure. There was never a need to manually move the train forward, unlike the case of fixed-frequency testing Ref. [22].

As discussed before, the fluctuation can be reduced with other approaches. A variable capacitor can be used in a receiving coil so that the resonance, and the effective impedance can be tuned electronically. This will change the field distribution on the array, and thus the power coupled to the receiver. When two resonant receivers are used and the received power is combined after rectification, the overall efficiency can be improved with much less fluctuation at different locations on the track.

It is worth to mention that the numerical and experimental study presented in this session were intended for general demonstration. The resonators in this study were not fully optimized. This can be a very flexible and powerful wireless power delivery solution. The resonators in the array does not have to be identical; they can be shaped to allow a curved or even forked track that may have loops or stub ends. With a particular application in mind, the design, size, and other parameters of the resonator array can be further optimized for better wireless power delivery.

2.4 Conclusion

In summary, we presented metamaterial-based technologies to improve near-field WPT in range, efficiency, and flexibility in this chapter. Two principal concepts and their implementations were discussed. First, using a properly designed metamaterial slab between two coils, the coupling between coils can be enhanced and the power transfer efficiency can be improved. Studies showed that significant efficiency improvement can still be achieved with reasonable material loss in metamaterials. In experiment, a metamaterial slab has been designed for a WPT system operating at 27 MHz, and the power transfer efficiency when the metamaterial slab is used is almost three times as high as the system without the slab. Second, resonant coupling-based WPT can be extended using an array of coupled resonators. The range of efficient power transfer is significantly increased using multiple coupled resonators in the array system. While conventional WPT technologies are mostly feasible only for static devices, the array-based system can be used to transfer power dynamically to mobile or loosely located devices as well. The array-based system has been studied analytically and numerically; experiment has been done to build an array of 30 resonant coils coupled by a single feeding antenna, and provide wireless power continuously to a train on the move. With the development of these technologies, the capability of near-field coupling-based WPT can be largely expanded, which potentially leads to new application areas.

References

1. Shimokura, N., Kaya, N., Shinohara, M., Matsumoto, H.: Point-to-point microwave power transmission experiment. *Electr. Eng. Jpn.* **120**(1), 33–39 (1997)
2. Cota (<http://www.ossia.com/cota/>); Energous (<http://www.energous.com/>)
3. Schuder, J.C., Stephenson, H.E., Townsend, J.F.: High-level electromagnetic energy transfer through a closed chest wall. *Inst. Radio Eng. Int. Conv. Rec.* **9**, 119 (1961)
4. Low, Z.N., Chinga, R.A., Tseng, R., Lin, J.: Design and test of a high-power high-efficiency loosely coupled planar wireless power transfer system. *IEEE Trans. Ind. Electron.* **56**, 1801 (2009)
5. Elliott, G.A.J., Raabe, S., Covic, G.A., Boys, J.T.: Multiphase pickups for large lateral tolerance contactless power-transfer systems. *IEEE Trans. Ind. Electron.* **57**, 1590 (2010)
6. de Donaldson, N., Perlins, T.A.: Analysis of resonant coupled coils in the design of radio frequency transcutaneous links. *Med. Biol. Eng. Comput.* **21**, 612 (1983)
7. Puers, R., Schuylenbergh, K.V., Catrysse, M., Hermans, B.: Wireless inductive transfer of power and data. In: *Analog Circuit Design*, p. 395. Springer (2006)
8. Kurs, A., Karalis, A., Moffatt, R., Joannopoulos, J.D., Fisher, P., Soljic, M.: Wireless power transfer via strongly coupled magnetic resonances. *Science* **317**, 83 (2007)
9. Valtchev, S., Borges, B., Brandisky, K., Klaassens, J.B.: Resonant contactless energy transfer with improved efficiency. *IEEE Trans. Power Electron.* **24**(3), 685–699 (2009)
10. Cannon, B.L., Hoburg, J.F., Stancil, D.D., Goldstein, S.C.: Magnetic resonant coupling as a potential means for wireless power transfer to multiple small receivers. *IEEE Trans. Power Electron.* **24**, 1819 (2009)

11. Yuan, Q., Chen, Q., Li, L., Sawaya, K.: Numerical analysis on transmission efficiency of evanescent resonant coupling wireless power transfer system. *IEEE Trans. Antennas Propag.* **58**(5), 1751–1758 (2010)
12. Sample, A.P., Meyer, D.T., Smith, J.R.: Analysis, experimental results, and range adaptation of magnetically coupled resonators for wireless power transfer. *IEEE Trans. Ind. Electron.* **58**, 544 (2011)
13. Kurs, A., Moffatt, R., Soljacic, M.: Simultaneous mid-range power transfer to multiple devices. *Appl. Phys. Lett.* **96**, 044102 (2010)
14. Wang, B., Nishino, T., Teo, K.H.: Wireless power transmission efficiency enhancement with metamaterials. In: *Proceedings of the IEEE International Conference on Wireless Information Technology and Systems (ICWITS'10)*, Honolulu, Hawai'i, 28 Aug–03 Sept 2010
15. Urzhumov, Y., Smith, D.R.: Metamaterial-enhanced coupling between magnetic dipoles for efficient wireless power transfer. *Phys. Rev. B* **83**, 205114 (2011)
16. Wang, B., Teo, K.H., Nishino, T., Yerazunis, W., Barnwell, J., Zhang, J.: Wireless power transfer with metamaterials. In: *Proceedings of European Conference on Antennas and Propagation (EuCAP 2011)*, 11–15 Apr 2011, Rome, Italy
17. Wang, B., Teo, K.H., Nishino, T., Yerazunis, W., Barnwell, J., Zhang, J.: Experiments on wireless power transfer with metamaterials. *Appl. Phys. Lett.* **98**, 254101 (2011)
18. Wang, B., Teo, K.H.: Metamaterials for wireless power transfer. In: *Proceedings of IEEE International Workshop on Antenna Technology (iWAT)*, 5–7 Mar 2012, Tuson, Arizona (2012)
19. Huang, D., Urzhumov, Y., Smith, D.R., Teo, K.H., Zhang, J.: Magnetic superlens-enhanced inductive coupling for wireless power transfer. *J. Appl. Phys.* **111**, 64902 (2012)
20. Wang, B., Teo, K.H., Yamaguchi, S., Takahashi, T., Konishi, Y.: Flexible and mobile near-field wireless power transfer using an array of resonators. *IEICE Technical Report, WPT2011-16* (2011)
21. Wang, B., Ellstein, D., Teo, K.H.: Analysis on wireless power transfer to moving devices Based on array of resonators. In: *Proceedings of European Conference on Antennas and Propagation (EuCAP) 2012*, 26–30 Mar 2012, Prague, Czech Republic
22. Yerazunis, W., Wang, B., Teo, K.H.: Power delivery optimization for a mobile power transfer system based on resonator arrays. In: *Proceedings of International Symposium on Antennas and Propagation (ISAP) 2012*, 29 Oct–2 Nov 2012, Nagoya, Japan
23. Lipworth, G., Ensworth, J., Seetharam, K., Huang, D., Lee, J.S., Schmalenberg, P., Nomura, T., Reynolds, M.S., Smith, D.R., Urzhumov, Y.: Magnetic metamaterial superlens for increased range wireless power transfer. *Sci. Rep.* **4**, 3642 (2014)
24. Rajagopalan, A., RamRakhyani, A.K., Schurig, D., Lazzi, G.: Improving power transfer efficiency of a short-range telemetry system using compact metamaterials. *IEEE Trans. Microwave Theory Tech.* **62**, 947–955 (2014)
25. Ranaweera, A.L.A.K., Moscoso, C.A., Lee, J.-W.: Anisotropic metamaterial for efficiency enhancement of mid-range wireless power transfer under coil misalignment. *J. Phys. D: Appl. Phys.* **48**, 455104 (2015)
26. Zhang, Y., Tang, H., Yao, C., Li, Y., Xiao, S.: Experiments on adjustable magnetic metamaterials applied in megahertz wireless power transmission. *AIP Adv.* **5**, 017142 (2015)
27. Pendry, J.B.: Negative refraction makes a perfect lens. *Phys. Rev. Lett.* **85**, 3966 (2000)
28. Shelby, R.A., Smith, D.R., Schultz, S.: Experimental verification of a negative index of refraction. *Science* **292**, 77–79 (2001)
29. Smith, D.R., Pendry, J.B., Wiltshire, M.C.K.: Metamaterials and negative refractive index. *Science* **305**, 788 (2004)
30. Fang, N., Lee, H., Sun, C., Zhang, X.: Sub-diffraction-limited optical imaging with a silver superlens. *Science* **308**, 534 (2005)
31. Schurig, D., Mock, J.J., Justice, B.J., Cummer, S.A., Pendry, J.B., Starr, A.F., Smith, D.R.: Metamaterial electromagnetic cloak at microwave frequencies. *Science* **314**, 977 (2006)
32. Engheta, N., Ziolkowski, R.W.: A positive future for double-negative metamaterials. *IEEE Trans. Microw. Theory Tech.* **53**, 1535 (2005)

33. Freire, M.J., Marques, R., Jelinek, L.: Experimental demonstration of a $\mu = -1$ metamaterial lens for magnetic resonance imaging. *Appl. Phys. Lett.* **93**, 231108 (2008)
34. Smith, D.R., Schultz, S., Markos, P., Soukoulis, C.M.: Determination of effective permittivity and permeability of metamaterials from reflection and transmission coefficients. *Phys. Rev. B* **65**, 195104 (2002)
35. Freire, M.J., Marques, R.: Planar magnetoinductive lens for three-dimensional subwavelength imaging. *Appl. Phys. Lett.* **86**, 182505 (2005)
36. Ellstein, D., Wang, B., Teo, K.H.: Accurate models for spiral resonators. In: *Proceedings of European Microwave Week (EuMW 2012)*, 28 Oct–2 Nov 2012, Amsterdam, Netherlands

Wireless Power Transfer Algorithms, Technologies and
Applications in Ad Hoc Communication Networks

Nikoletseas, S.; Yang, Y.; Georgiadis, A. (Eds.)

2016, XVIII, 745 p. 356 illus., 230 illus. in color.,

Hardcover

ISBN: 978-3-319-46809-9